

**Comparison of the 3ω Method and Time-Domain Thermorefectance
for Measurements of the Cross-plane Thermal Conductivity of Epitaxial
Semiconductors**

*Yee Kan Koh¹, Suzanne L. Singer², Woochul Kim³, Joshua M.O. Zide⁴, Hong Lu⁵, David
G. Cahill¹, Arun Majumdar², Arthur C. Gossard⁵*

*¹Department of Materials Science and Engineering, and Frederick Seitz Materials
Research Laboratory, University of Illinois, Urbana, Illinois 61801, USA*

*²Department of Mechanical Engineering, University of California, Berkeley, CA 94720,
USA*

³School of Mechanical Engineering, Yonsei University, Seoul, Korea

*⁴Department of Electrical and Computer Engineering, University of Delaware, Newark,
DE 19716, USA*

⁵Materials Department, University of California, Santa Barbara, CA 93106, USA

The 3ω technique and time-domain thermorefectance (TDTR) are two experimental methods capable of measuring the cross-plane thermal conductivity of thin films. We compare the cross-plane thermal conductivity measured by the 3ω method and TDTR on epitaxial $(\text{In}_{0.52}\text{Al}_{0.48})_x(\text{In}_{0.53}\text{Ga}_{0.47})_{1-x}\text{As}$ alloy layers with embedded ErAs nanoparticles. Thermal conductivities measured by TDTR at low modulation frequencies (~ 1 MHz) are typically in good agreement with thermal conductivities measured by the 3ω method. We

discuss the accuracy and limitations of both methods and provide guidelines for estimating uncertainties for each approach.

I. INTRODUCTION

The cross-plane thermal conductivity of thin films is a critical property that impacts the performance of semiconductor devices,^{1,2} phase change memory,^{3,4} thermal barrier coatings^{5,6} and thermoelectric modules.⁷ Although many techniques have been developed to measure the thermal conductivity of thin films, currently the 3ω method⁸ is one of the most widely used because of its low cost, simplicity, and high accuracy. Applications of the 3ω method to electrically conducting or semiconducting materials can be challenging, however, because of the need to electrically isolate the metal test pattern from the sample. This additional layer of electrical insulation inevitably introduces an additional thermal resistance between the metal test pattern and the sample which can reduce both the sensitivity and accuracy of the technique.

Because of these challenges, we have recently developed a new experimental approach with the ability to measure thermal conductivity of electrically conducting thin films that is based on modulated time-domain thermoreflectance (TDTR). Measurements of the picosecond to nanosecond time evolution of surface temperature by thermoreflectance—i.e., the change in the reflectivity of a metal produced by changes in temperature—have been used for over two decades in studies of thermal transport in materials. The terminology is not always unique or consistent but the term “time-domain thermoreflectance” (TDTR)^{9,10} typically refers to approaches based on pump-probe

methods and mode-locked laser oscillators. (Approaches based on heating by Q-switched nanosecond laser pulses and temperature measurements by cw lasers are typically referred to as “transient thermoreflectance.”) Because of our recent advances in both the experimental design and methods for data analysis, TDTR is now a flexible and accurate tool for measuring the thermal conductivity of bulk and thin film materials that span a range in thermal conductivities from the lowest thermal conductivities ever observed in a fully dense solid¹¹ to the high thermal conductivities of pure metals.¹² The approach has been thoroughly validated on a wide range of materials and thin films with known thermal conductivity.^{12,13}

Applications of TDTR to epitaxial semiconductor alloys, however, also face challenges because the thermal penetration depth used in the experiment is of the same order-of-magnitude as the mean-free-paths of phonons that are important in heat conduction. (The thermal penetration depth d is the spatial extent of the temperature gradient; for heat flow in one-dimension and a modulated heat source of angular frequency ω , $d = \sqrt{D/\omega}$, D is the thermal diffusivity.) A complete description of the relevant physics is given in Ref. 14 but the essential problem is that the differential equations used to analyze the TDTR data are not rigorously valid when a significant fraction of the heat-carrying phonons have mean-free-paths λ that are greater than d . Strictly speaking, temperature gradient and thermal conductivity cannot be defined under these conditions. However, an *apparent* thermal conductivity can still be derived from the analysis of TDTR measurements. The conclusion of our prior work is that phonons with $\lambda > d$ do not contribute to the thermal conductivity measured in the TDTR experiment. This difficulty is essentially confined to measurements of semiconductor alloys because

the strong frequency dependence of phonon scattering by substitutional atoms produces a situation where a significant fraction of the thermal conductivity is controlled by a small fraction of the acoustic phonons of the crystal.

In our approach for analyzing TDTR data, most of the sensitivity to the thermal conductivity arises from the out-of-phase signal and the modulation frequency f of the pump beam determines d . Since typically, $0.3 < f < 10$ MHz in TDTR; using $D = 3 \times 10^{-2} \text{ cm}^2 \text{ s}^{-1}$ as a thermal diffusivity characteristic of semiconductor alloys, gives $0.2 < d < 1.3 \text{ } \mu\text{m}$. The 3ω method uses much lower modulation frequencies, $0.1 < f < 10$ kHz, and the thermal penetrations depths are much longer than the mean-free-paths of all of the heat carrying phonons. We can expect, therefore, that measurements of the thermal conductivity of semiconductor alloys by TDTR and the 3ω method could show differences, particularly if a high modulation frequency is used in the TDTR experiment or when phonons with long mean-free-paths are particularly important contributors to heat conduction. Our prior studies suggest, however, that readily accessible modulation frequencies on the order of 1 MHz, are sufficient to satisfy the condition $d > \lambda$ for the heat carrying phonons in a semiconductor alloy and we can expect that the measurements by TDTR and the 3ω method will converge in the limit of low modulation frequency. The purpose of this paper is to test these expectations by directly comparing thermal conductivity data acquired by the 3ω method and TDTR on the same set of samples. Experiments using the 3ω method were performed at University of California at Berkeley and experiments using TDTR were performed at University of Illinois at Urbana-Champaign.

II. EXPERIMENTAL DETAILS

A. 3ω Method

In 3ω measurements, a narrow metal line (often Au or Pt with Cr or Ti as the adhesion layer) of ~ 400 nm thickness and ~ 30 μm width is patterned on a sample. Electrical current i of frequency ω is applied to the metal line with electrical resistance r , generating joule heating of $i^2 r$ within the metal line with a frequency component at 2ω . As a result of this oscillating heat source, a temperature oscillation and a corresponding resistance oscillation at frequency 2ω are induced in the metal line. Hence, a component of the voltage oscillation ($v=ir$) across the metal line contains a third harmonic, 3ω . The thermal conductivity of the sample can be deduced from this 3ω voltage oscillation.

The differential 3ω method is frequently employed^{15,16} in measurements of the thermal conductivity of thin films. A reference sample without the thin film of interest is prepared simultaneously with the sample containing the film of interest such that the metal line patterned on both samples has the same thickness and width. Both the thin film sample and the reference are measured using similar heating power and the same range of heater frequencies. The temperature drop across the thin film ΔT_f can then be derived from the difference in the amplitude of the temperature oscillation of the sample ΔT_S and the reference ΔT_R ; $\Delta T_f / P_S = \Delta T_S / P_S - \Delta T_R / P_R$, where P_S and P_R are the heating power of the sample and the reference, respectively. Assuming that the penetration depth is much larger than the thickness of the film, which is almost always the case for the 3ω method, and assuming good thermal contact between the metal pattern and the thin film, the cross-plane thermal conductivity of the thin film Λ_f is given by

$$\Lambda_f = \frac{P_S h_f}{2b'l\Delta T_f} \quad (1)$$

where h_f is the thin film thickness, b and l are the half-width and the length of the metal line, and $2b' = 2b + 0.76h_f$ is an effective linewidth¹⁷ that takes into account lateral heat flow in an isotropic thin film.

Equation 1 is rigorously valid only if the film is much thinner than the width of the metal line and heat flow is approximately one-dimensional through the thickness of the film. Furthermore, the effective linewidth used in Eq. 1 is accurate only if the thermal conductivity of the substrate Λ_s is much larger than Λ_f . Hence, for a relatively thick film with a small contrast between the thermal conductivity of the film and the substrate, an exact solution of two dimensional heat flow in layered structures¹⁸ should be employed instead of the approximation given by Eq. 1. For a typical experiment on a semiconductor thin film with $h_f = 5 \mu\text{m}$, $\Lambda_f = 5 \text{ W m}^{-1} \text{ K}^{-1}$, $\Lambda_s = 40 \text{ W m}^{-1} \text{ K}^{-1}$, $b = 15 \mu\text{m}$, and $f = 1 \text{ kHz}$, the error is $\approx 6\%$. As the semiconductor samples reported in this paper are only $1 - 2 \mu\text{m}$ thick, we use Eq. 1 in our data analysis; the error incurred due to this estimation is $\approx 1\%$.

Applicability of the differential 3ω method to measurements of the cross-plane thermal conductivity of thin films is often limited by a few constraints. First, the metal line has to be electrically isolated from the film. Thus, if the film is electrically conductive, a thin layer of dielectric—e.g., a 180 nm thick film of a-SiO₂—must be deposited prior to the deposition of the metal line to avoid leakage of electric current through the sample and the generation of spurious third-harmonic signals. Second, as noted above, the differential 3ω method is only suitable for films with thermal conductivity much lower than the thermal conductivity of the substrate. Third, to keep the

uncertainty of the differential 3ω method within an acceptable range, the temperature drop across the film should be larger than both the temperature drop across the dielectric layer and the temperature drop within the substrate. If we assume that the relative uncertainty in measurements of the temperature drops δM is approximately the same for the sample and the reference, the uncertainty in the thermal conductivity $\delta\Lambda_{3\omega}$ is

$$\delta\Lambda_{3\omega} = \frac{\sqrt{(\Delta T_R)^2 + (\Delta T_S)^2}}{\Delta T_f} \delta M \quad (2)$$

For a typical δM of $\sim 10\%$, $\delta\Lambda_{3\omega} \approx 22\%$ if the temperature drop in the thin film and the reference sample is the same, i.e., $\Delta T_f = \Delta T_R$, comparable to the uncertainty estimated in Ref. 17. However, uncertainty analysis here is not based on independently measured parameters unlike the one in Ref. 17. So, this gives a rough estimation on the uncertainty. Since measurements with uncertainty larger than 25% are not very useful, $\Delta T_f = \Delta T_R$ can be used to set the minimum film thickness, $h_{\min}^{3\omega}$, measurable using the differential 3ω method. We emphasize that this minimum film thickness is a measure of whether the film is thermally thick enough for 3ω measurements and depends heavily on the thermal properties of the samples.

ΔT_f depends linearly on the thickness h_f and thermal conductivity Λ_f of the film, but ΔT_R is a more complicated nonlinear function of the thickness h_d and the thermal conductivity Λ_d of the dielectric, the thermal conductivity Λ_s of the substrate and other experimental parameters such as the half-width of the metal line b and the heating frequency f . Fortunately, the nonlinear portion of ΔT_R does not change significantly for typical values of material properties and experiment parameters. Hence, by setting $\Delta T_f = \Delta T_R$ and using common values for the other parameters, we find

$$h_{\min}^{3\omega} = \frac{\Lambda_f}{\Lambda_d} h_d + \frac{\Lambda_f}{\Lambda_s} b \quad (3)$$

For a typical measurement of the thermal conductivity of a semiconductor alloy, this minimum film thickness is on the order of microns. For example, for $\Lambda_f = 5 \text{ W m}^{-1} \text{ K}^{-1}$, $\Lambda_s = 50 \text{ W m}^{-1} \text{ K}^{-1}$, $h_d = 150 \text{ nm}$, $\Lambda_d = 1.0 \text{ W m}^{-1} \text{ K}^{-1}$, and $b = 15 \text{ }\mu\text{m}$, then $h_{\min}^{3\omega} \approx 2 \text{ }\mu\text{m}$.

We measure all samples, except for an $\text{In}_{0.53}\text{Ga}_{0.47}\text{As}$ sample embedded with 3% ErAs, using the differential 3ω method as described above. For the $\text{In}_{0.53}\text{Ga}_{0.47}\text{As}$ sample embedded with 3% ErAs, we employ the traditional 3ω method as described in Ref. 19. For the analysis of this sample, we determine the thickness of the SiO_2 thin film from microspectrophotometry and estimate the thermal conductivity of the SiO_2 film from the bulk value of $1.4 \text{ W m}^{-1} \text{ K}^{-1}$. The uncertainty of the 3ω measurement for the sample is $\approx 25\%$.

B. Time Domain Thermoreflectance

We do not describe the details of our TDTR equipment and approach here, but refer the readers to Ref. 20. In TDTR measurements, the output of a mode-locked laser oscillator is split into a pump beam and a probe beam, with the relative delay time between the pump and probe pulses being adjusted by a mechanical stage. Samples are heated by the pump beam, which is modulated by an electro-optic modulator at frequency f , $0.1 < f < 10 \text{ MHz}$. The temperature at the surface of the sample is monitored by the probe beam. For measurements using TDTR, a thin layer ($\sim 80 \text{ nm}$) of metal with high thermoreflectance (e.g., Al) is deposited on the sample and serves as the transducer to absorb the heating pump beam and to convert the temperature excursions at the surface into changes in the intensity of the reflected probe beam. A photodiode and a lock-in

amplifier are used to measure the small changes in the probe intensity that are created by the pump. These changes in reflected intensity at frequency f have both an in-phase V_{in} and out-of-phase component V_{out} . We analyze the ratio V_{in}/V_{out} to make use of the additional information in the out-of-phase signal and eliminate artifacts created by unintended variations in the diameter or position of the pump beam created by the optical delay line.

The thermal penetration depth of TDTR measurements d_{TDTR} is given by

$$d_{TDTR} = \sqrt{D_f / \pi f} \quad (4)$$

where $D_f = \Lambda_f / C_f$ is the thermal diffusivity of the thin film, Λ_f and C_f are the thermal conductivity and the volumetric heat capacity of the film. For a film of $\Lambda_f = 5 \text{ W m}^{-1} \text{ K}^{-1}$, $C_f = 1.5 \text{ J cm}^{-3} \text{ K}^{-1}$ and $f = 10 \text{ MHz}$, $d_{TDTR} \approx 300 \text{ nm}$. Usually, the penetration depth in TDTR is much smaller than the $1/e^2$ radii of the laser beams of a several microns. Hence, heat flow in TDTR is predominantly one dimensional through the thickness of the film.

Data analysis in TDTR is more complicated than the 3ω method. Measurements of the ratios V_{in}/V_{out} as a function of delay time are compared to numerical solutions of a thermal model.²¹ The thermal model normally has two free parameters: the thermal conductance of the Al/film interface and Λ_f of the thin film. For most cases, we are able to separate these two parameters from the fitting of the model calculations to the measurements.^{4,13,14}

We estimate the heat capacity of $(\text{In}_{0.52}\text{Al}_{0.48})_x(\text{In}_{0.53}\text{Ga}_{0.47})_{1-x}\text{As}$ digital alloys used in the thermal model from the composition-weighted average of the heat capacity of bulk InAs, AlAs and GaAs. As the concentration of ErAs is relatively low ($<3\%$), we ignore

the effects of embedment of ErAs nanoparticles to the heat capacity of the $(\text{In}_{0.52}\text{Al}_{0.48})_x(\text{In}_{0.53}\text{Ga}_{0.47})_{1-x}\text{As}$ matrix.

To evaluate the limits of applicability of TDTR, we calculate the sensitivity of our experiments to various parameters used in the measurements. We define sensitivity parameters S_α as

$$S_\alpha = \frac{\partial \ln R}{\partial \ln \alpha} \quad (5)$$

where R is the absolute value of the ratio of in-phase and out-of-phase of the lock-in amplifier and α is the parameter in the thermal model, e.g., the thickness h_f , thermal conductivity Λ_f of the thin films, or the thickness of the Al transducer h_{Al} . In addition to these parameters, another important uncertainty in TDTR measurements is the absolute value of the phase of the reference channel of the lock-in amplifier ϕ . For a small change in the absolute value of the phase, $\Delta\phi$, the ratio R transforms into a new value R' according to

$$R' = R \left(1 + \Delta\phi \left(R + \frac{1}{R} \right) \right) \quad (6)$$

The sensitivity of TDTR measurements to the absolute value of the phase is

$$S_\phi = \frac{\partial \ln R}{\partial \phi} = R + \frac{1}{R} \quad (7)$$

Sensitivity parameters for modulation frequencies f of 10 MHz and 0.6 MHz are summarized in Fig. 1. The film thickness at which a TDTR measurement is most sensitive to the thermal conductivity of the film is when the film thickness is comparable to thermal penetration depth, $h_f \approx d_{\text{TDTR}}$. At $f = 10$ MHz, TDTR measurements are sensitive to the thermal conductivity of thin films down to thickness of ~ 60 nm. Hence,

TDTR is capable of measuring thermal conductivity of films much thinner than the 3ω method. As discussed below, for high modulation frequencies, the uncertainty in determining the phase is usually small; thus the accuracy of TDTR measurements at high frequencies is limited by the uncertainty in determining the thickness of the metal transducer film. In most cases, we use Al and measure the thickness of the Al film by picosecond acoustics. The relatively low melting point of Al makes Al unsuitable for high temperature measurements; Pt is much more refractory than Al and has adequate thermoreflectance but we have not been able to use the standard approaches of picosecond acoustics to measure the Pt film thickness. Instead, we use Rutherford backscattering (RBS) or an extension of picosecond acoustics we recently implemented in our lab, time-domain pump-beam-deflection,²² to determine the thickness of the Pt films. The accuracy in determining the thickness of the metal film is $\approx 3\%$ and an overall accuracy of $\approx 7\%$ is usually achieved in TDTR measurements at $f = 10$ MHz. The choice of metal transducer film does not affect the thermal conductivity measured by TDTR.

At a relatively low modulation frequency of $f = 0.6$ MHz, TDTR measurements are only sensitive to the thermal conductivity of the thin film if the film is sufficiently thick, see Fig. 1b. The accuracy of the thermal conductivity measured by TDTR at $f = 0.6$ MHz is primarily limited by the uncertainty in determining the phase. As the out-of-phase signal of the lock-in amplifier should not change across the zero time, we set the absolute value of the phase by adjusting the phase value in the reference channel of the lock-in amplifier until no significant difference is observed between the out-of-phase signal before and after zero delay time. The uncertainty in determining the phase $\delta\phi$ is controlled by the noise in the out-of-phase signal and can be estimated from

$$\delta\phi = \frac{\delta V_{out}}{\Delta V_{in}} \quad (11)$$

where δV_{out} is the rms noise in the out-of-phase signal and ΔV_{in} is the jump in the in-phase signal at zero time.

In our apparatus, the noise is dominated by the fluctuations in the probe laser intensity within a narrow bandwidth around the modulation frequency f ; thus, noise in the out-of-phase signal δV_{out} is proportional to the laser power. ΔV_{in} , on the other hand, is proportional to the square of the laser power. (The signal arises from the product of the pump and probe powers.) As a result, the uncertainty in the phase is inversely proportional to the laser power. Since the steady-state temperature rise ΔT is proportional to the laser power, the product of $\delta\phi$ and ΔT can be used as a figure of merit for how the uncertainty of the phase changes with modulation frequency.

The product of $\delta\phi$ and ΔT is plotted in Fig. 2 as a function of modulation frequency f for two typical samples coated with Al and Pt. We find that the uncertainty in determining the phase is relatively small at $f > 1$ MHz, but deteriorates rapidly as f is reduced below 1 MHz. We typically limit the temperature rise to ~ 10 K. Hence, $\delta\phi \approx 1.5$ mrad at $f = 10$ MHz and $\delta\phi \approx 20$ mrad at $f = 0.6$ MHz; the corresponding uncertainties in thermal conductivity due to $\delta\phi$ are 1.5% and 12%, respectively.

In principle, the uncertainty in the phase $\delta\phi$ at low modulation frequencies can be reduced with the use of a pulse-picker that reduces the repetition rate of the laser oscillator.¹⁴ For fixed laser power, and a reduction of the repetition rate from 80 to 5 MHz, the uncertainty in the phase $\delta\phi$ can be reduced by an order of magnitude. The challenge of using of a pulse-picker in TDTR measurements is to properly account for the

energy in the optical pulses that leak through the pulse picker. We used a pulse-picker in our prior work but not in the new results presented here.

C. Sample Preparation

Samples used for comparison are $(\text{In}_{0.52}\text{Al}_{0.48})_x(\text{In}_{0.53}\text{Ga}_{0.47})_{1-x}\text{As}$ epitaxial layers with embedded ErAs nanoparticles grown on InP substrates by molecular beam epitaxy (MBE).²³ The thin films are 1 – 2 μm thick, with ErAs nanoparticles of concentration 0 – 3% randomly distributed in the $(\text{In}_{0.52}\text{Al}_{0.48})_x(\text{In}_{0.53}\text{Ga}_{0.47})_{1-x}\text{As}$ matrices. Samples without ErAs nanoparticle embedment are doped with $5 \times 10^{18} \text{ cm}^{-3}$ Si. The $(\text{In}_{0.52}\text{Al}_{0.48})_x(\text{In}_{0.53}\text{Ga}_{0.47})_{1-x}\text{As}$ matrices are digital alloys, i.e., superlattices of $\text{In}_{0.53}\text{Ga}_{0.47}\text{As}$ and $\text{In}_{0.52}\text{Al}_{0.48}\text{As}$ with very short periods of a few monolayers. For the 3 ω method measurements, a SiO_2 layer of ~ 180 nm thick is deposited on the samples, followed by Pt deposition (~ 380 nm thick) with Cr (~ 4 nm thick) as an adhesion layer. Lithographic patterning and etching creates a Pt metal line ~ 30 μm wide.

III. RESULTS AND DISCUSSION

In Fig. 3a, we plot the cross-plane thermal conductivity of 2 μm $(\text{In}_{0.52}\text{Al}_{0.48})_x(\text{In}_{0.53}\text{Ga}_{0.47})_{1-x}\text{As}$ films doped with 0.3% ErAs measured by TDTR at modulation frequencies of 0.6 and 10 MHz. As discussed above, the accuracy of TDTR measurements is $\approx 7\%$ at $f = 10$ MHz and $\approx 12\%$ at $f = 0.6$ MHz. The data acquired using $f = 10$ MHz are $\approx 30\%$ lower than measurements at $f = 0.6$ MHz, consistent with our previous work on semiconductor alloys.¹⁴

For a thick film with moderate thermal conductivity, TDTR essentially measures the thermal effusivity $(\Lambda_f C_f)^{1/2}$ of the film. As a result, a distribution of phonons with small total heat capacity do not contribute to the thermal conductivity measured by TDTR if these phonons have long mean-free-paths and are not thermalized within the thermal penetration depth.¹⁴ By varying the penetration depth, the frequency dependence of TDTR measurements is a probe of the distribution of phonon mean-free-paths. For example, the data plotted in Fig. 3a suggest that phonons with mean-free-paths in the range 300-1000 nm contribute $\sim 1 \text{ W m}^{-1} \text{ K}^{-1}$ to the thermal conductivity of epitaxial $(\text{In}_{0.52}\text{Al}_{0.48})_x(\text{In}_{0.53}\text{Ga}_{0.47})_{1-x}\text{As}$ films with 0.3% ErAs nanoparticles.

We compare the TDTR measurements at $f = 0.6 \text{ MHz}$ to measurements by the 3ω method on the same samples in Fig. 3b. The accuracy of the 3ω measurements is estimated to be 20%. Measurements of TDTR at $f = 0.6 \text{ MHz}$ are in good agreement with measurements using the 3ω method. Measurements by both methods indicate that the thermal conductivity of $(\text{In}_{0.52}\text{Al}_{0.48})_x(\text{In}_{0.53}\text{Ga}_{0.47})_{1-x}\text{As}$ does not vary significantly with the percentage of $\text{In}_{0.52}\text{Al}_{0.48}\text{As}$. We also compare our new measurements to the thermal conductivity of $\text{In}_{0.53}\text{Ga}_{0.47}\text{As}$ film doped with 0.3% ErAs as reported by Kim *et al.*⁶ using the 3ω method, see Fig. 4a. Kim's measurement is $\approx 25 \%$ less than our new data. This discrepancy could be due to higher uncertainty in the 3ω method when applied to thinner films. We estimate the uncertainty to be $\approx 30\%$ for this sample, as indicated in Fig. 4a.

The inclusion of ErAs nanoparticles produces a clear reduction in the thermal conductivity of $\text{In}_{0.53}\text{Ga}_{0.47}\text{As}$, see Fig. 4a, but we do not observe a significant difference in the TDTR measurements of the room-temperature thermal conductivity of $(\text{In}_{0.52}\text{Al}_{0.48})_{0.2}(\text{In}_{0.53}\text{Ga}_{0.47})_{0.8}\text{As}$ epitaxial films with and without doping of 0.3% ErAs,

see Fig. 4b. The difference measured by the 3ω method is $\approx 25\%$. Although there may be some percentage variation on the ErAs concentration on the samples from the nominal 0.3%, this variation is expected to be small. In previous work,⁷ even significantly smaller concentrations of ErAs (0.075 at%) resulted in a significant reduction in thermal conductivity of $\text{In}_{0.53}\text{Ga}_{0.47}\text{As}$. Hence, the reduction in thermal conductivity by ErAs nanoparticles in $(\text{In}_{0.52}\text{Al}_{0.48})_x(\text{In}_{0.53}\text{Ga}_{0.47})_{1-x}\text{As}$ is much less significant than in $\text{In}_{0.53}\text{Ga}_{0.47}\text{As}$. This result is expected because of the additional phonon scattering by the high density of interfaces in $(\text{In}_{0.52}\text{Al}_{0.48})_x(\text{In}_{0.53}\text{Ga}_{0.47})_{1-x}\text{As}$ digital alloys.

We plot the frequency-dependent thermal conductivity measured by TDTR as a function of penetration depth for three $\text{In}_{0.53}\text{Ga}_{0.47}\text{As}$ samples in Fig. 5a and three $(\text{In}_{0.52}\text{Al}_{0.48})_{0.2}(\text{In}_{0.53}\text{Ga}_{0.47})_{0.8}\text{As}$ samples in Fig. 5b. Data points in Fig. 5 are labelled by percentage of ErAs; two of the $(\text{In}_{0.52}\text{Al}_{0.48})_{0.2}(\text{In}_{0.53}\text{Ga}_{0.47})_{0.8}\text{As}$ samples (2 μm thick) and two of the $\text{In}_{0.53}\text{Ga}_{0.47}\text{As}$ samples (1.27 μm and 2 μm thick) are doped with 0.3% ErAs, while the other $\text{In}_{0.53}\text{Ga}_{0.47}\text{As}$ film (1.17 μm thick) is doped with 3% ErAs. For comparison, we plot our previous results for the frequency-dependent thermal conductivity of a 3.3 μm $\text{In}_{0.53}\text{Ga}_{0.47}\text{As}$ film¹⁴ (without ErAs doping) as dashed lines.

The frequency dependence of the TDTR measurements is strongest in an $\text{In}_{0.53}\text{Ga}_{0.47}\text{As}$ film without ErAs doping and weakest in an $\text{In}_{0.53}\text{Ga}_{0.47}\text{As}$ film with 3% doping, see Fig. 5a. Stronger frequency dependence in $\text{In}_{0.53}\text{Ga}_{0.47}\text{As}$ without ErAs suggests that phonons with intermediate mean-free-paths (300 – 1000 nm) play a more important role in the thermal transport. We consider the frequency dependence of thermal conductivity of $\text{In}_{0.53}\text{Ga}_{0.47}\text{As}$ and estimate that phonons with intermediate mean-free-path (300 – 1000 nm) contribute $\sim 3 \text{ W m}^{-1} \text{ K}^{-1}$ to the thermal conductivity of epitaxial

$\text{In}_{0.53}\text{Ga}_{0.47}\text{As}$ films. As the ErAs concentration is increased, phonons with intermediate mean-free-paths are scattered by ErAs nanoparticles, resulting in less frequency dependence. The results are consistent with the theory developed by Kim and Majumdar.²⁴

IV. CONCLUSIONS

Thermal conductivity measurements of semiconductor alloys by TDTR and the 3ω method agree to within experimental uncertainties if a low modulation frequency (~ 1 MHz) is used in TDTR. For TDTR, the experimental uncertainty is dominated by uncertainties in the thickness of the Al film transducer when the modulation frequency is high, $f = 10$ MHz, and is dominated by uncertainties in setting the phase for low modulation frequencies, $f = 0.6$ MHz; typical uncertainties are $\sim 7\%$ at $f = 10$ MHz and $\sim 12\%$ at $f = 0.6$ MHz. For the 3ω method, the uncertainty depends on the thickness and thermal conductivity of the thin film of interest. The frequency dependence of the thermal conductivity as measured by TDTR indicates that doping of 3% ErAs is sufficient to scatter most of the phonons in $\text{In}_{0.53}\text{Ga}_{0.47}\text{As}$ that have intermediate mean-free-paths.

ACKNOWLEDGMENTS

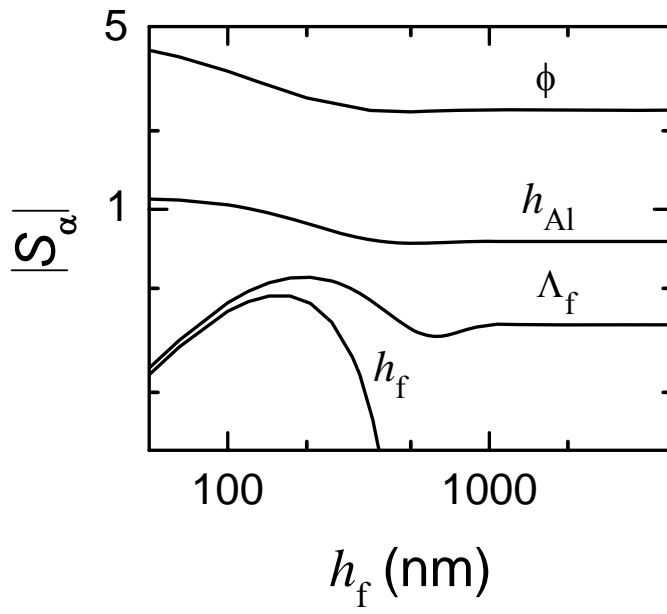
This work was supported by ONR Grant No. N00014-07-1-0190 and ONR Multidisciplinary University Research Initiative (MURI). Sample characterization used the facilities of the Center of Microanalysis of Materials which is partially supported by the U.S. Dept. of Energy under Grant No. DEFG02-91ER45439; and Laser Facility of the Frederick Seitz Materials Research Laboratory (MRL) at UIUC.

REFERENCES

-
- ¹ S.-M. Lee and D. G. Cahill, J. Appl. Phys. **81**, 2590 (1997).
- ² Y. K. Koh, Y. Cao, D. G. Cahill, and D. Jena, submitted.
- ³ E.-K. Kim, S.-I. Kwun, S.-M. Lee, H. Seo, and J.-G. Yoon, Appl. Phys. Lett. **76**, 3864 (2000).
- ⁴ H.-K. Lyeo, D. G. Cahill, B.-S. Lee, J. R. Abelson, M.-H. Kwon, K. B. Kim, S. G. Bishop, and B.-K. Cheong, Appl. Phys. Lett. **89**, 151904 (2006).
- ⁵ D. G. Cahill, S.-M. Lee, and T. I. Selinder, J. Appl. Phys. **83**, 5783 (1998).
- ⁶ R. M. Costescu, D. G. Cahill, F. H. Fabreguette, Z. A. Sechrist, and S. M. George, Science **303**, 989 (2004).
- ⁷ W. Kim, J. Zide, A. Gossard, D. Klenov, S. Stemmer, A. Shakouri, and A. Majumdar, Phys. Rev. Lett. **96**, 045901 (2006).
- ⁸ D. G. Cahill and R. O. Pohl, Phys. Rev. B **35**, 4067 (1987).
- ⁹ C. A. Paddock and G. L. Eesley, J. Appl. Phys. **60**, 285 (1986).
- ¹⁰ D. A. Young, C. Thomsen, H. T. Grahn, H. J. Maris, and J. Tauc, in *Phonon Scattering in Condensed Matter*, edited by A. C. Anderson and J. P. Wolfe (Springer, Berlin, 1986), p. 49.
- ¹¹ C. Chiritescu, D. G. Cahill, N. Nguyen, D. Johnson, A. Bodapati, P. Keblinski, and P. Zschack, Science **315**, 351 (2007)
- ¹² J.-C. Zhao, X. Zheng, and D. G. Cahill, Materials Today **8** (10), 28 (2005).
- ¹³ R. M. Costescu, M. A. Wall, and D. G. Cahill, Phys. Rev. B **67**, 054302 (2003).
- ¹⁴ Y. K. Koh and D. G. Cahill, Phys. Rev. B **76**, 075207 (2007).

-
- ¹⁵ R. Venkatasubramanian, *Phys. Rev. B* **61**, 3091 (2000).
- ¹⁶ T. Borca-Tasciuc, W. Liu, J. Liu, T. Zeng, D. W. Song, C. D. Moore, G. Chen, K. L. Wang, M. S. Goorsky, T. Radetic, R. Gronsky, T. Koga, and M. S. Dresselhaus, *Superlattices Microstruct.* **28**, 199 (2000).
- ¹⁷ D. T. Borca-Tasciuc, A. R. Kumar, and G. Chen, *Rev. Sci. Instrum.* **72**, 2139 (2001).
- ¹⁸ J. H. Kim, A. Feldman, and D. Novotny, *J. Appl. Phys.* **86**, 3959 (1999).
- ¹⁹ D. G. Cahill, M. Katiyar, and J. R. Abelson, *Phys. Rev. B*, **50**, 6077 (1994).
- ²⁰ D. G. Cahill, W. K. Ford, K. E. Goodson, G. D. Mahan, A. Majumdar, H. J. Maris, R. Merlin, and S. R. Phillpot, *J. Appl. Phys.* **93**, 793 (2003).
- ²¹ D. G. Cahill, *Rev. Sci. Instrum.* **75**, 5119 (2004).
- ²² X. Zheng, D. G. Cahill, R. Weaver, J.-C. Zhao, submitted.
- ²³ J. M. Zide, D. O. Klenov, S. Stemmer, A. C. Gossard, G. Zeng, J. E. Bowers, D. Vashaee, and A. Shakouri, *Appl. Phys. Lett.* **87**, 112102 (2005).
- ²⁴ W. Kim and A. Majumdar, *J. Appl. Phys.* **99**, 084306 (2006).

a)



b)

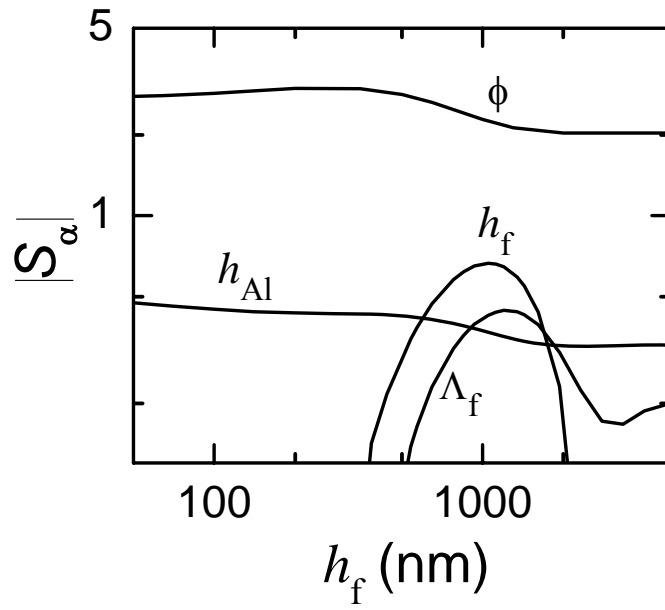


FIG. 1. Absolute value of the sensitivity parameter S_α of the TDTR ratio signal (ratio of the in-phase and out-of-phase signals of the rf lock-in amplifier) at modulation frequencies (a) $f = 10$ MHz and (b) $f = 0.6$ MHz for a hypothetical sample consisting of an Al transducer layer with thickness $h_{Al} = 100$ nm; a thin film with thermal conductivity $\Lambda_f = 5 \text{ W m}^{-1} \text{ K}^{-1}$, heat capacity $C_f = 1.5 \text{ J cm}^{-3} \text{ K}^{-1}$ and thickness h_f ; a substrate with $\Lambda_s = 50 \text{ W m}^{-1} \text{ K}^{-1}$ and $C_s = 1.5 \text{ J cm}^{-3} \text{ K}^{-1}$; and an interface thermal conductance between the Al transducer layer and the film of $G = 100 \text{ MW m}^{-2} \text{ K}^{-1}$. Each curve is labeled by the corresponding parameter in the thermal model; ϕ is the phase of the reference channel of the rf lock-in amplifier.

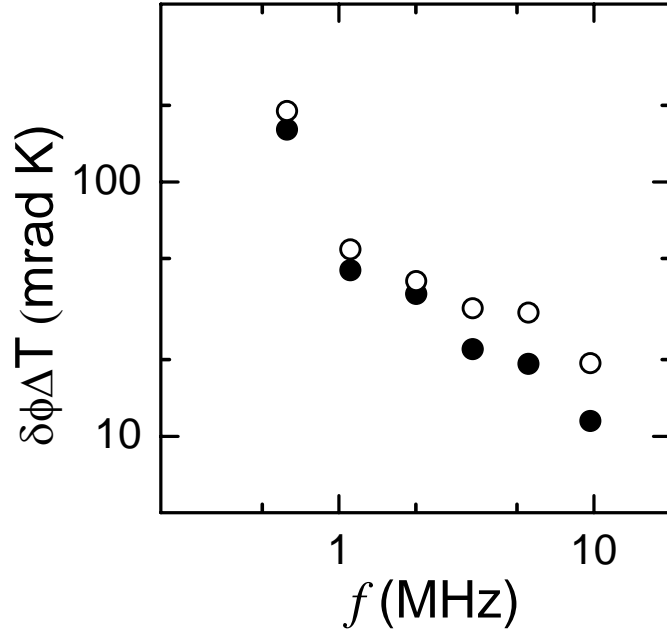
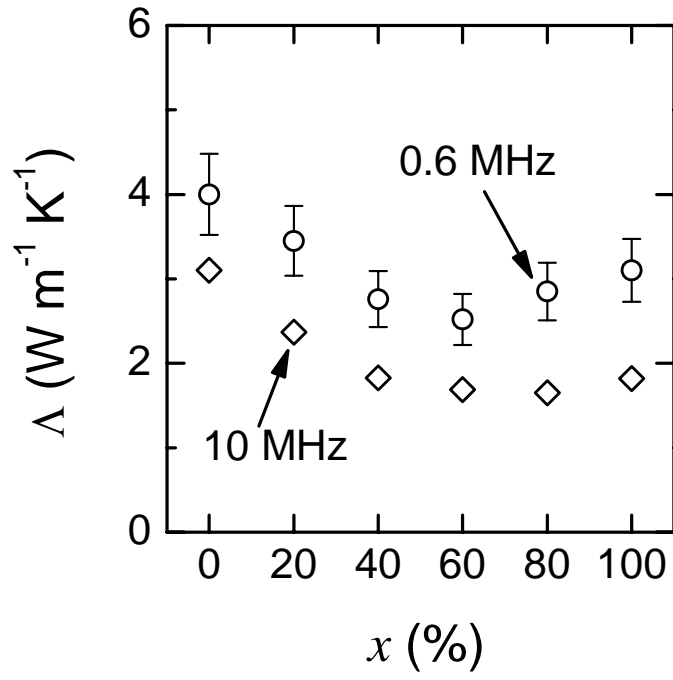


FIG. 2. The product of steady-state temperature rise ΔT and the uncertainty in setting the absolute value of the phase of the reference channel of the rf lock-in amplifier $\delta\phi$, as a function of modulation frequency f . The data in figure were measured on an Al-coated 1.17 μm thick $\text{In}_{0.53}\text{Ga}_{0.47}\text{As}$ layer doped with 3% ErAs (solid circles) and a Pt-coated 2 μm thick $\text{In}_{0.53}\text{Ga}_{0.47}\text{As}$ doped with 0.3% ErAs (open circles).

a)



b)

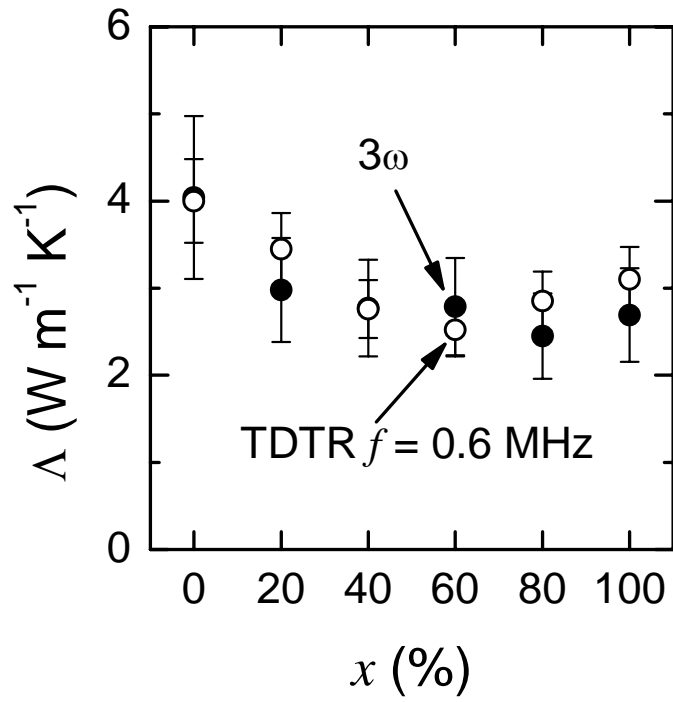
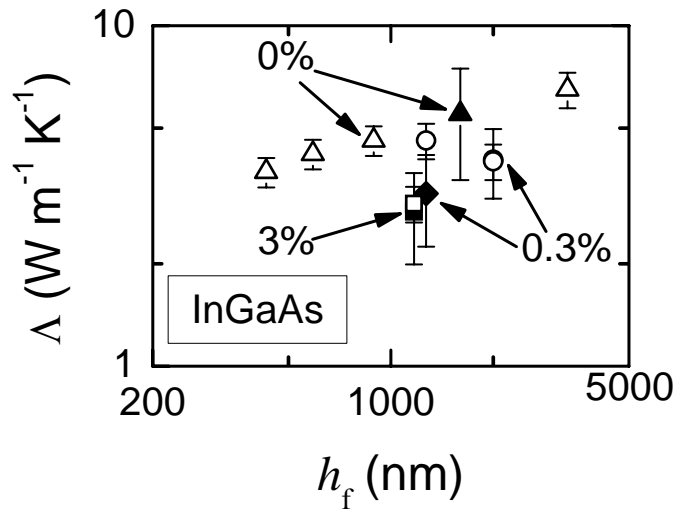


FIG. 3. (a) Comparison of thermal conductivity measurements by TDTR at a modulation frequencies of $f = 10$ MHz (open diamonds) and 0.6 MHz (open circles), on 2 μm thick $(\text{In}_{0.52}\text{Al}_{0.48})_x(\text{In}_{0.53}\text{Ga}_{0.47})_{1-x}\text{As}$ layers with 0.3% ErAs doping. The uncertainty of TDTR measurements at $f = 0.6$ MHz is about the size of the symbols and the error bars are omitted for clarity. (b) Comparison of thermal conductivity of the same samples measured by the 3ω method (solid circles) and TDTR at $f = 0.6$ MHz (open circles). For $x = 0\%$ and 40%, TDTR and the 3ω method measurements essentially identical. TDTR measurements at $f = 0.6$ MHz agree within experimental uncertainty with measurements by the 3ω method.

a)



b)

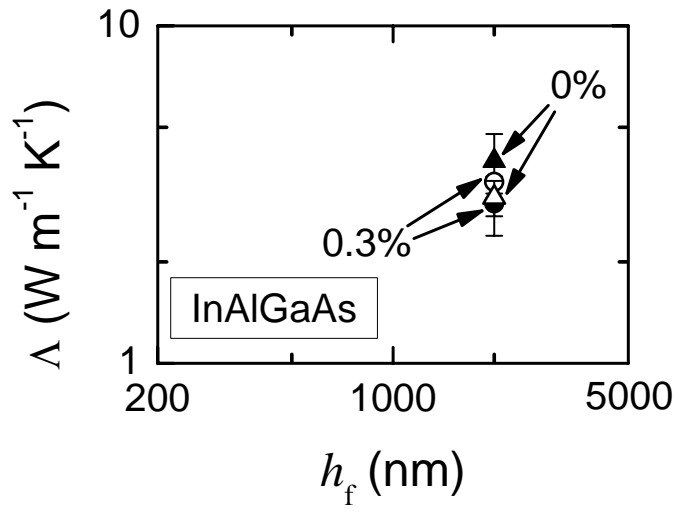


FIG. 4. (a) Thermal conductivity of $\text{In}_{0.53}\text{Ga}_{0.47}\text{As}$ with 0.3% (circles) and 3% (squares) ErAs doping measured by TDTR at $f = 0.6$ MHz (open symbols) and the 3ω method (solid symbols) plotted as a function of film thickness h_f . Labels are percentage of ErAs. Measurements by TDTR (open circle) and the 3ω method (solid circle) on a $2 \mu\text{m}$ $\text{In}_{0.53}\text{Ga}_{0.47}\text{As}$ with 0.3% ErAs overlap. In the plot, prior 3ω measurements by Kim *et al.*⁷ on a $1.27 \mu\text{m}$ $\text{In}_{0.53}\text{Ga}_{0.47}\text{As}$ doped with 0.3% ErAs (solid diamond) and a $1.67 \mu\text{m}$ $\text{In}_{0.53}\text{Ga}_{0.47}\text{As}$ (solid triangle), and prior TDTR measurements at low modulation frequencies by Koh and Cahill¹⁴ on $\text{In}_{0.53}\text{Ga}_{0.47}\text{As}$ epitaxial films (open triangles) are included for comparison. (b) Thermal conductivity of $(\text{In}_{0.52}\text{Al}_{0.48})_{0.2}(\text{In}_{0.53}\text{Ga}_{0.47})_{0.8}\text{As}$ doped with (circles) and without (triangles) 0.3% ErAs. Open symbols are TDTR measurements while solid symbols are the 3ω measurements. Labels are the percentage of ErAs. The 3ω measurements indicate 25% reduction in Λ due to 0.3% doping of ErAs while TDTR measurements are essentially identical with and without ErAs doping.

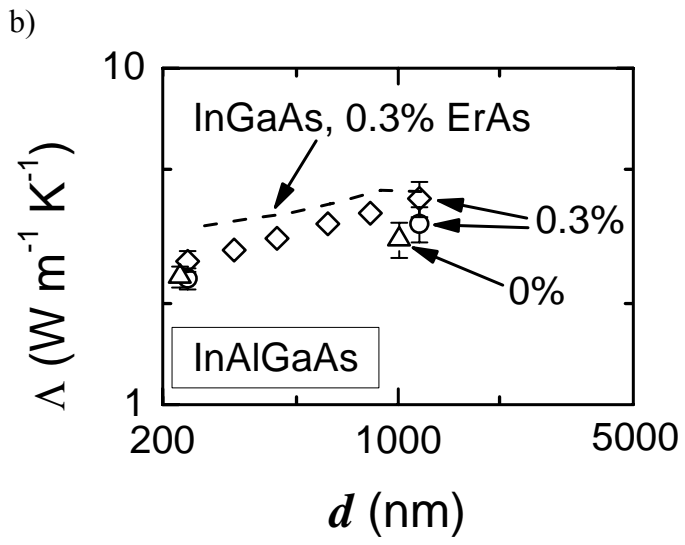
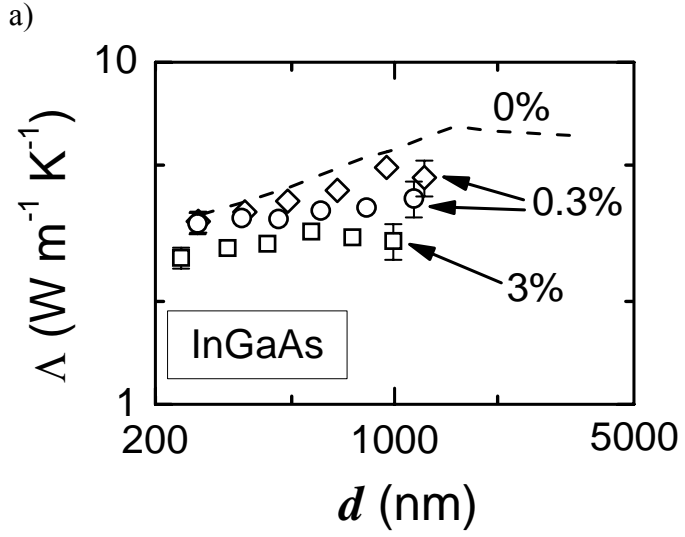


FIG. 5. (a) Frequency dependence of the thermal conductivity of $\text{In}_{0.53}\text{Ga}_{0.47}\text{As}$ films measured by TDTR plotted as a function of thermal penetration depth d . The data are for three samples: Al-coated $1.27\ \mu\text{m}$ $\text{In}_{0.53}\text{Ga}_{0.47}\text{As}$ doped with 0.3% ErAs (diamonds), Pt-coated $2\ \mu\text{m}$ $\text{In}_{0.53}\text{Ga}_{0.47}\text{As}$ doped with 0.3% ErAs (circles) and Al-coated $1.17\ \mu\text{m}$ $\text{In}_{0.53}\text{Ga}_{0.47}\text{As}$ doped with 3% ErAs (squares). The dashed line is frequency dependence of TDTR measurements on a $3.3\ \mu\text{m}$ $\text{In}_{0.53}\text{Ga}_{0.47}\text{As}$ film from Ref. 14. The labels are percentage of ErAs doping. (b) Frequency dependence of thermal conductivity of $2\ \mu\text{m}$ $(\text{In}_{0.52}\text{Al}_{0.48})_{0.2}(\text{In}_{0.53}\text{Ga}_{0.47})_{0.8}\text{As}$ films measured by TDTR plotted as a function of thermal penetration depth d . The data are for three samples: two films doped with 0.3% ErAs, coated with Al (open diamonds) and Pt (open circles); and one sample without ErAs doping coated with Pt (open triangles). Thermal conductivities of $\text{In}_{0.53}\text{Ga}_{0.47}\text{As}$ films with 0.3% ErAs measured by TDTR from part (a) are reproduced here as the dashed line.